

Microscopic Identification of a Bimolecular Reaction Intermediate

Hiroshi Uetsuka, Akira Sasahara, Akira Yamakata, and Hiroshi Onishi*

Kanagawa Academy of Science and Technology, KSP East 404, Takatsu-ku, Kawasaki, Kanagawa 213-0012, Japan

Received: June 6, 2002

How a molecule impinging from an ambient phase attaches to and reacts with a preadsorbed reactant was studied by scanning tunneling microscopy (STM). A carboxylate (RCOO^-) chemisorbed on a $\text{TiO}_2(110)$ surface was exchanged by another carboxylate ($\text{R}'\text{COO}^-$) via an $\text{S}_{\text{N}}2$ -like mechanism when the RCOO^- -covered TiO_2 surface was exposed to $\text{R}'\text{COOH}$ vapor at room temperature or below. An $\text{R}'\text{COOH}$ impinging from the gas phase was temporarily bound to a preadsorbed RCOO^- yielding a bimolecular intermediate. The trapped $\text{R}'\text{COOH}$ was inserted into the monolayer and dissociated to produce an adsorbed $\text{R}'\text{COO}^-$. One of the carboxylates (RCOO^- or $\text{R}'\text{COO}^-$) was then pushed out of the monolayer to restore the intermediate and released to the vapor phase. The individual reaction steps were resolved using time-lapse imaging.

Introduction

A reactant once adsorbed on a solid surface is usually assumed to react without aid of chemical species from an ambient (gas or liquid) phase. The reactant is transferred to the same product at the same rate regardless of the ambient when its concentration at the surface is identical. Many examples have been found to justify this simplified assumption. On the other hand, reaction kinetics over heterogeneous catalysts sometimes indicate that a molecule impinging from the ambient phase reacts with the preadsorbed reactant.^{1,2} Such ambient-driven reactions are expected to play an important role in biological, geological, meteorological, and astronomical interfaces surrounded by various atmospheres, as well as in industrial applications (catalysis, thin film growth, etc). There is thus a strong need to determine how an ambient-phase molecule attaches to a preadsorbed reactant and forms a bimolecular intermediate complex. However, this is often difficult to determine experimentally, especially by spectroscopic methods, because a very small quantity of the proposed complex is present in a dense atmosphere.

Scanning tunneling microscopy (STM) with single-molecule detectability is promising for this purpose. In-situ STM has provided rich information in relation to where and how individual reaction steps take place on semiconductors³ and on metals.⁴ Previous STM studies, however, focused on the reaction of preadsorbed reactants without the aid of ambient molecules as assumed in the simplified picture. The present paper reports the first microscopic identification of an intermediate complex composed of a preadsorbed reactant and a molecule impinging from the ambient. The target reaction is the exchange of molecules between the vapor and adsorbed phases at a gas–solid interface. It is a most simple reaction catalyzed on a solid surface and models the material transport across a gas–solid interface. Molecule exchange at a liquid–solid interface was microscopically observed by using a substituted long alkane as a tracer, although the intermediate state of the exchange was not detected.⁵

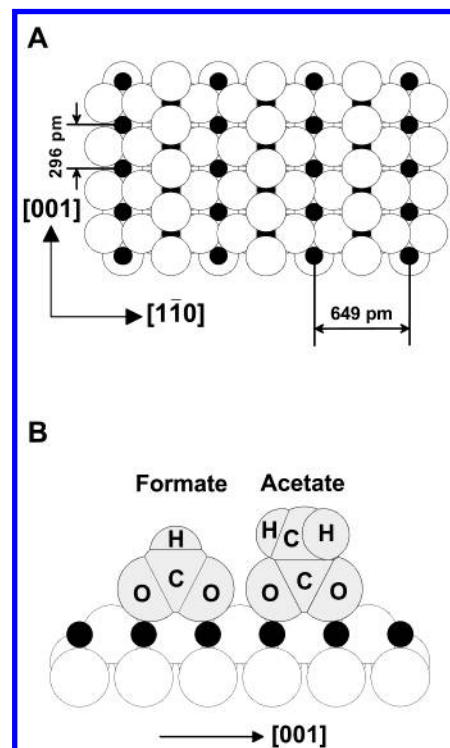


Figure 1. The schematic views of (A) the $\text{TiO}_2(110)$ surface, and (B) the chemisorbed formate and acetate. The constituent atoms are presented as spheres of their van der Waals or ionic radius. The protons dissociated from the parent acids are not shown.

A single crystalline wafer of rutile $\text{TiO}_2(110)$ was employed as the substrate. The electrostatic (Madelung) potential corrugated over the ionic surface restricts the two-dimensional migration of the adsorbates.⁶ The top-layer structure shown in Figure 1(A) is accepted as the nonreconstructed (1×1) phase.⁷ When the TiO_2 surface is exposed to formic acid (HCOOH) vapor at room temperature, an acid molecule is dissociated to a bridge-adsorbed formate (HCOO^-) and a proton. Photoelectron diffraction,⁸ vibrational spectroscopy,^{9,10} STM,¹¹ and theoretical¹² studies evidenced the bridge configuration as illustrated in Figure 1(B). The dissociative adsorption is suspended when

* Author to whom correspondence should be addressed. Phone: +81-44-819-2048. Fax: +81-44-819-2095. E-mail: oni@net.ksp.or.jp.

all the Ti atoms are occupied by the bridge formates. The yielded formate monolayer is stable under the vacuum and ordered in a (2×1) periodicity.¹³ The ionic bonds between the adsorbate and substrate are sufficiently stable to maintain the bridge configuration of the acetate (CH_3COO^-) adsorbed on this surface.^{14,15} The different STM topographies of the formate and acetate are utilized to trace the exchange reaction in the present study.

Experimental Section

Experiments were performed using an ultrahigh-vacuum-compatible microscope (JEOL, JSPM-4500S) with a liquid- N_2 Dewar bottle for sample cooling. A one-side polished $\text{TiO}_2(110)$ wafer ($6.5 \times 1 \times 0.35 \text{ mm}^3$, Earth Chemicals) was back-coated with a nickel film for resistive heating. The (1×1) phase of $\text{TiO}_2(110)$ was prepared with cycles of argon ion sputtering and vacuum annealing at 900 K.¹⁶ The (1×1) surface was exposed to formic acid vapor for several Langmuirs ($1 \text{ L} = 10^{-6} \text{ Torr s}$) at room temperature in a preparation chamber separated from the microscope stage by a gate valve. The formate-covered surface was cooled to 150 K on the microscope stage and resistively warmed at desired temperatures. A platinum resistance thermometer (Sensycon, GR2105) was clamped with the TiO_2 wafer to achieve precise control of the temperature. A constant current topography of 512×512 pixels was sequentially observed at an acquisition rate of 6 s/frame with an electrochemically etched tungsten tip in the presence or absence of CH_3COOH vapor.

Results and Discussion

Molecule exchange between the gas and adsorbate phases frequently occurred at room temperature when the formate-covered $\text{TiO}_2(110)$ surface was exposed to CH_3COOH vapor of $1 \times 10^{-7} \text{ Pa}$ which was brought into the microscope chamber at $t = 0$. Panels (A) and (B) in Figure 2 show the constant-current topography of the same area observed at $t = 215$ and 491 s. Two species of different brightnesses covered the surface. The number of bright molecules increased with the exposure time, whereas the number of nonbright molecules decreased to compensate for the increment of the bright molecules. The complementary variations indicate that the bright and nonbright molecules are the acetate and formate, respectively. The (2×1) order of the carboxylates was not disturbed at any acetate/formate ratio. This evidenced that the two carboxylates were bridge-adsorbed in the mixed-monolayers. A finite contribution of CH_3 -derived molecular orbitals to the tip-surface tunneling was expected to enhance the microscope topography. An image enhancement of acetate over formate was observed on $\text{Cu}(110)$.¹⁷ Ninety-nine formates were exchanged during a 276 s period from frame (A) to (B). The exchange frequency was estimated at $3.6 \times 10^{11} \text{ events cm}^{-2} \text{ s}^{-1}$ by assuming a constant rate of exchange, while the impinging frequency of CH_3COOH molecules as ideal gas of $1 \times 10^{-7} \text{ Pa}$ was estimated to be $8 \times 10^{11} \text{ cm}^{-2} \text{ s}^{-1}$. The comparison of the two frequencies led to an exchange reaction probability of 0.5. The gas pressure was measured by an ion gauge 15 cm from the microscope stage. The local pressure on the wafer beneath the tip was unknown. Hence, the figure provided a rough estimate for the probability.

The acetate adsorption on an unoccupied Ti-atom pair, and the subsequent desorption of a formate at an independent location provided an $\text{S}_{\text{N}}1$ mechanism for the exchange reaction. However, only a limited number of unoccupied sites were available at the surface on which the replacement steadily occurred as shown in Figure 2. The number of vacant sites

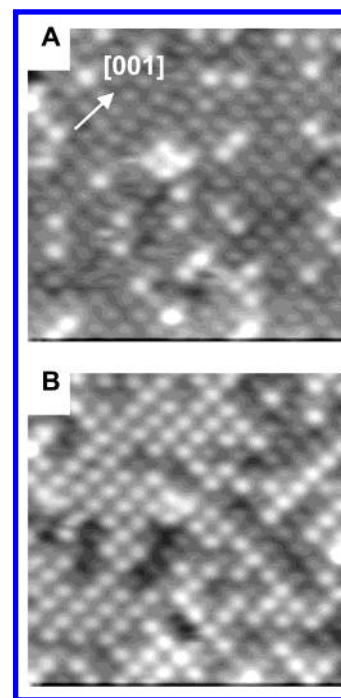
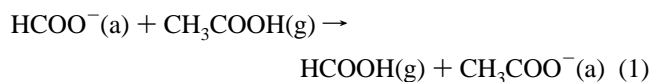


Figure 2. The STM topography of a formate monolayer on $\text{TiO}_2(110)$ being exchanged by acetates. A formate-covered surface maintained at room temperature was exposed to CH_3COOH vapor at $t = 0$. Frames (A) and (B) were observed at $t = 215$ and 491 s in the presence of the atmosphere. Image size: $10 \times 10 \text{ nm}^2$, sample bias voltage (V_s): +1.0 V, tunneling current (I_t): 0.4 nA.

identified as dark patches in the topography was (A) 2 and (B) 1 as a Ti-atom pair. The reaction mechanism via such a small quantity (ca. 1% of the monolayer density) of vacancies cannot be responsible for a major share of the frequent replacement. Instead, a $\text{S}_{\text{N}}2$ -like mechanism,



was strongly suggested where a CH_3COOH molecule impinging from the gas-phase reacted with the very HCOO^- to be replaced.

A bimolecular intermediate complex through which the proposed reaction 1 proceeded was identified in time-lapse imaging performed at lower temperatures. A $\text{TiO}_2(110)$ surface covered by a mixture of chemisorbed formate and acetate was cooled at 187 K and exposed to CH_3COOH vapor of $6 \times 10^{-7} \text{ Pa}$ for 1500 s. Acid molecules condensed on the monolayer presented unresolved topography of vague shapes. The exposed surface was then heated at 193 K to evaporate the condensed material. Figure 3 shows two sequential images observed on the surface at 193 K. A third species 0.04 nm taller than the acetate appeared in frame (A). We attribute it to a bimolecular intermediate complex composed of a preadsorbed acetate and an excess CH_3COOH bound to it. Six protrusions on the solid line in (A) were identified in the cross section (C) as formate 1 (F_1), formate 2 (F_2), acetate 1 (A_1), intermediate (I) including acetate 2 (A_2), and an excess CH_3COOH (E), acetate 3 (A_3), and acetate 4 (A_4). In frame (B) obtained 6 s later than (A), one chemisorbed acetate (A_5) newly appeared at the cost of one I. Seven particles were resolved as F_1 , F_2 (as a shoulder of A_1), A_1 , A_5 , A_2 , A_3 , and A_4 . A_5 was tentatively assigned to the particle between A_1 and A_2 as shown in the cross section (D), though the identity of the three molecules (A_1 , A_5 , and A_2) is unknown. The observed transformation of the topography cannot

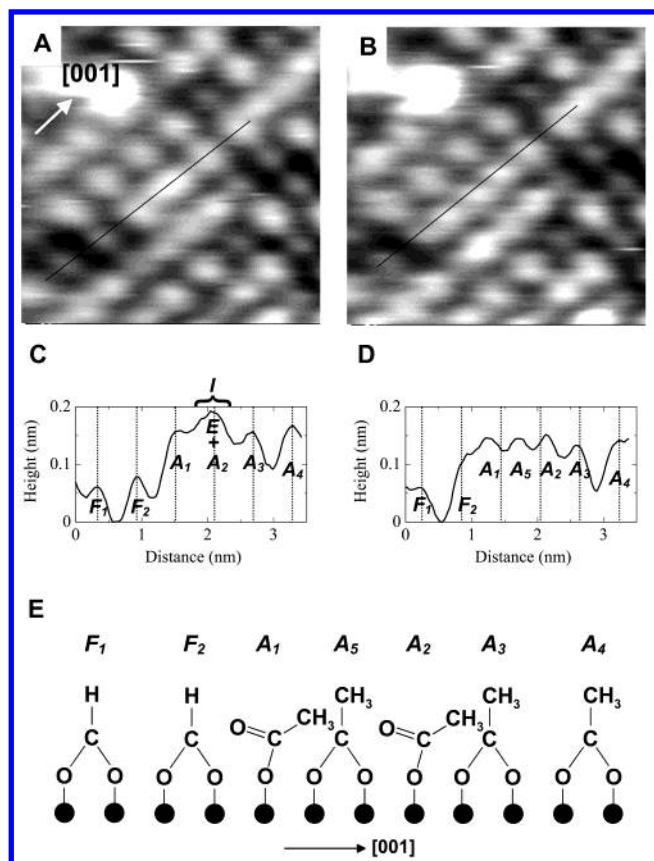


Figure 3. The time-lapse STM observation of an acetate inserted in a chemisorbed monolayer of carboxylates. A TiO₂(110) surface covered by chemisorbed formates and acetates was cooled at 187 K and exposed to CH₃COOH vapor of 6×10^{-7} Pa for 1500 s. Frames (A) and (B) were recorded at an interval of 6 s on the exposed surface heated at 193 K in the vacuum. Image size: 5×5 nm², V_s : +1.1 V, I_t : 0.4 nA. The cross sections determined on lines in (A) and (B) are shown in (C) and (D), respectively. The broken lines in (C) and (D) present the sites to be occupied by carboxylates ordered in the (2×1) periodicity. The proposed mechanism of the insertion is illustrated in (E).

be interpreted with the simple desorption of the excess CH₃COOH in I, because A₁ laterally shifted toward F₂. Instead, we propose that the excess CH₃COOH was inserted into the chemisorbed monolayer and was dissociated to yield A₅. Two of the three acetates (A₁, A₅, and A₂) should have been adsorbed in a monodentate geometry to make room for A₅, as illustrated in panel (E). The monodentate form of the carboxylates bound to one metal atom is known to exist on ZnO(0001)–Zn,¹⁸ NiO(111),¹⁹ and TiO₂(111)²⁰ surfaces. The large bump in the upper left corner of Figure 3(A) is perhaps a particle of TiO_x. Similar particles were observed at the initial stage of the O₂-reoxidation of a reduced TiO₂(110) surface.²¹

The reverse step (the elimination of an acetate) was also traced on a separate location of the surface. Figure 4 presents three sequential pictures recorded at intervals of 6 s. In the initial state, five acetates (A₂–A₆) were adsorbed on the line of frame (A). In the following frame (B), one of the acetates (tentatively assigned to A₄) was pushed out of the monolayer to yield an intermediate (I). The protons released in the dissociation of the preadsorbed carboxylates are left on the surface at this low temperature¹³ and available for the recombinative elimination reaction. The excess CH₃COOH (E) in I either migrated or sublimated away, leaving four bridge-acetates (A₂, A₃, A₅, and A₆) in frame (C).

The intermediate formation was not a rare phenomenon. Ten intermediates and 50 inserted adsorbates were observed in a

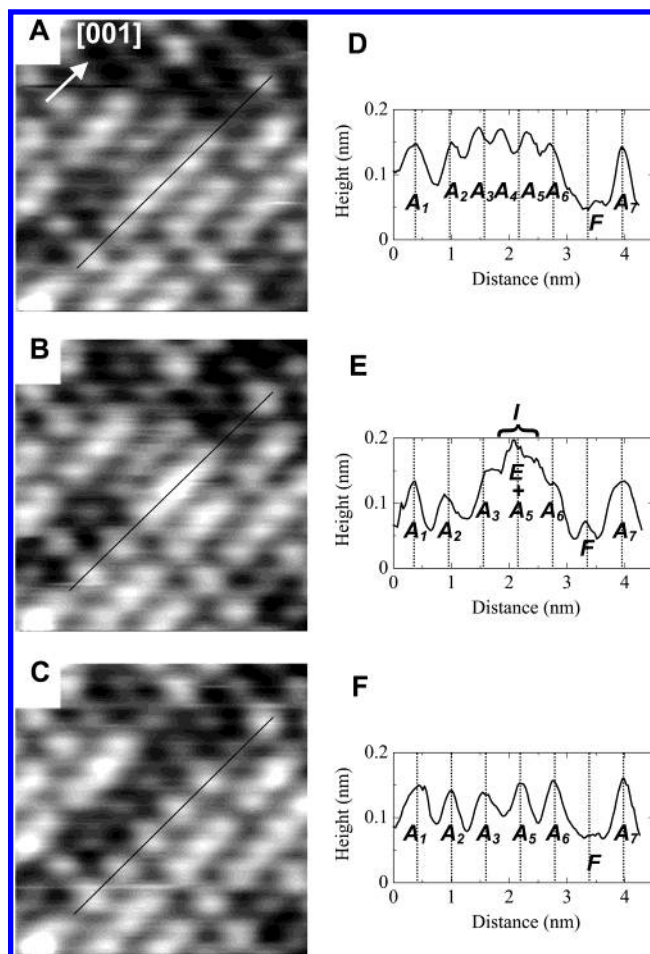


Figure 4. The time-lapse STM observation of the acetate elimination. Frames (A), (B), and (C) were recorded at intervals of 6 s on a different area of the surface in Figure 3. Image size: 5×5 nm², V_s : +1.1 V, I_t : 0.4 nA, surface temperature: 193 K. The cross sections determined on the lines in (A), (B), and (C) are presented in (D), (E), and (F). The broken lines show the sites to be occupied by (2×1) -ordered carboxylates.

typical image of 342 nm² obtained at 193 K, showing that they could not be assigned to impurities such as water. In addition, the observed transformations (formation and consumption) of the bimolecular intermediate were accompanied by the complementary expulsion and production of one adsorbed acetate as shown in Figures 3 and 4. This supports the proposed composition of one excess CH₃COOH in a complex.

The overall exchange reaction 1 is completed when the insertion and elimination steps consecutively occur at the same location. The rates of the steps are much more accelerated at room-temperature reducing the residence time of the intermediate complex and inserted adsorbates. Those short-lived states are beyond the time resolution of our microscope (0.1 s/molecule), being consistent with their absence in the sequential topography observed at room temperature (Figure 2).

The excess CH₃COOH in the intermediate complex was fixed on the carboxylate to be replaced. Its residence time averaging over several observations was more than 30 s at 193 K. It was necessary to distinguish such an immobilized state from the physisorbed state. HCOOH physisorbed on TiO₂(100)–(1 × 3) desorbs at 180–220 K in an ultrahigh vacuum.²² A significant coverage of physisorbed CH₃COOH was expected on the surface exposed to the atmosphere of 6×10^{-7} Pa. However, the physisorbed species should have been very mobile over the chemisorbed monolayer and was unlikely to be imaged at 193

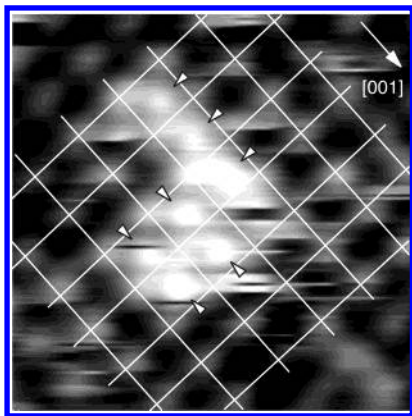
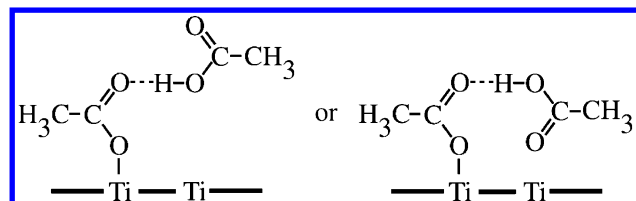


Figure 5. The STM topography of acetic acid molecules physisorbed on an acetate-covered $\text{TiO}_2(110)$ surface. A two-dimensional cluster of seven molecules marked by arrowheads was condensed on the surface exposed to CH_3COOH vapor of 2.1×10^{-8} Pa at 148 K. The white mesh shows the (2×1) order of the first-layer acetates. Image size: $5 \times 5 \text{ nm}^2$, V_s : +1.6 V, I_t : 0.4 nA.

K. Indeed, the physisorbed, second-layer molecules were able to be imaged by further cooling the surface. Figure 5 shows the STM topography of an acetate-saturated $\text{TiO}_2(110)$ surface placed in 2.1×10^{-8} Pa CH_3COOH vapor at 148 K. Seven bright particles overlying the monolayer were assigned to CH_3COOH molecules physisorbed and two-dimensionally clustered, while nonclustered molecules still mobile at this temperature were presented as fragment- or scratch-shaped images. The clustered molecules were adsorbed on the 4-fold hollow sites of the (2×1) -ordered acetates. Chemisorbed acetates inserted between a second-layer molecule and the ionic surface screened the electrostatic force causing the physisorption. The topography of the bimolecular complex I was, in contrast, centered at a position to be filled by an acetate ordered along the (2×1) mesh. The different appearance of the intermediate complex and physisorbed molecule proves that they are different species from each other. How the excess CH_3COOH is bound to the preadsorbed acetate remains to be determined. The microscope topography of the CH_3COOH –acetate complex in Figures 3 and 4 was only 0.04 nm taller than that of the neighboring acetates. The physisorbed, nonclustered CH_3COOH exhibited fragment-shaped topography 0.10 nm taller than that of the acetate. The reduced corrugation allows us to speculate that the excess CH_3COOH is partially inserted in the monolayer, though the constant-current topography does not always reproduce



physical topography of an adsorbate. The preadsorbed acetate may be transformed to a monodentate form and form a hydrogen bond with the excess CH_3COOH as a hydrogen-bonded bimolecular complex was proposed in the carboxylate exchange reaction on $\text{Ni}(110)$.²³

The role of the bimolecular complex in more complicated reactions is another open question. On the $\text{TiO}_2(110)$ surface placed in a vacuum, the formate unimolecularly decomposed to a CO and an adsorbed OH^- with an activation energy of 120 kJ/mol. The decomposition products switched to CO_2 and H_2 in a formic acid atmosphere accompanied with a reduction of activation energy to 15 kJ/mol, where the preadsorbed formate was proposed to react with a HCOOH from the gas phase.¹³ A HCOOH –formate complex analogous to I-state may possibly mediate the bimolecular decomposition reaction.

Acknowledgment. T. Matsumoto and J. Kubota are acknowledged for their advice in the use of the resistance thermometer. This work was partly supported by Grants-in-Aid (No. 13740409) from Japan Society for the Promotion of Science.

References and Notes

- (1) Iwasawa, Y. *Acc. Chem. Res.* **1997**, *30*, 103.
- (2) Tamaru, K. *Appl. Catal.* **1997**, *A 151*, 167.
- (3) Pelz, J. P.; Koch, R. H. *Phys. Rev.* **1990**, *B 42*, 3761.
- (4) Winterlin, J. *Adv. Catal.* **2000**, *45*, 131, and references therein.
- (5) Padowitz, D. F.; Messmore, B. W. *J. Phys. Chem.* **2000**, *B 104*, 9943.
- (6) Onishi, H.; Yamaguchi, Y.; Fukui, K.; Iwasawa, Y. *J. Phys. Chem.* **1996**, *100*, 9582.
- (7) Henrich, V. E.; Cox, P. A. *The Surface Science of Metal Oxides*; Cambridge University Press: New York, 1994.
- (8) Thevuthasan, S.; Herman, G. S.; Kim, Y. J.; Chambers, S. A.; Peden, C. H. F.; Wang, Z.; Ynzunza, R. X.; Tober, E. D.; Morais, J.; Fadley, C. S. *Surf. Sci.* **1998**, *401*, 261.
- (9) Henderson, M. A. *J. Phys. Chem.* **1997**, *B 101*, 221.
- (10) Hayden, B. E.; King, A.; Newton, M. A. *J. Phys. Chem.* **1999**, *B 103*, 203.
- (11) Onishi, H.; Iwasawa, Y. *Chem. Phys. Lett.* **1994**, *226*, 111.
- (12) Käckell, P.; Terakura, K. *Surf. Sci.* **2000**, *461*, 191.
- (13) Onishi, H.; Aruga, T.; Iwasawa, Y. *J. Catal.* **1994**, *146*, 557.
- (14) Guo, Q.; Cocks, I.; Williams, E. M. *J. Chem. Phys.* **1997**, *106*, 2924.
- (15) Gutierrez-Sosa, A.; Martinez-Escobedo, P.; Raza, H.; Lindsay, R.; Wincott, P. L.; Thornton, G. *Surf. Sci.* **2001**, *471*, 163.
- (16) Onishi, H.; Fukui, K.; Iwasawa, Y. *Bull. Chem. Soc. Jpn.* **1995**, *68*, 2447.
- (17) Silva, S. L.; Pham, T. M.; Patel, A. A.; Haq, S.; Leibsle, F. M. *Surf. Sci.* **2000**, *452*, 79.
- (18) Petrie, W.; Vohs, J. M. *Surf. Sci.* **1991**, *245*, 315.
- (19) Bandara, A.; Kubota, J.; Wada, A.; Domen, K.; Hirose, C. *J. Phys. Chem.* **1997**, *B 101*, 361.
- (20) Uetsuka, H.; Henderson, M. A.; Onishi, H. In preparation.
- (21) Onishi, H.; Iwasawa, Y. *Phys. Rev. Lett.* **1996**, *76*, 791.
- (22) Henderson, M. A. *J. Phys. Chem.* **1995**, *99*, 15253.
- (23) Yamakata, A.; Kubota, J.; Kondo, J. N.; Hirose, C.; Domen, K. *J. Phys. Chem.* **1998**, *B 102*, 4401.